Quantitative Validation Assessment on Shorelines Extracted from Image Classification Techniques of Medium Resolution Satellite Images Based on Change Analysis

Syaifulnizam Abd Manaf[1], Norwati Mustapha[1], Md Nasir Sulaiman[1], Nor Azura Husin[1], Helmi Zulhaidi Mohd Shafri[2] and Mohd Radzi Abdul Hamid[3]

[1] *Intelligent Computing Research Group, Faculty of Computer Science and Information Technology, Universiti Putra Malaysia*

[2] *Geospatial Information Science Research Centre, Faculty of Engineering, Universiti Putra Malaysia*

[3] *Coastal Management and Oceanography Research Centre, National Hydraulic Research Institute of Malaysia*

nizamkpt2020@gmail.com

***Abstract*— Shoreline extraction provides the boundary information of land and water, which helps monitor erosions or accretions of coastal zones. Such monitoring can be performed by using satellite images rather than by using traditional ground survey. To date, shorelines can be extracted from satellite images with a high degree of accuracy by using satellite image classification techniques based on machine learning, which helps identify the land and water classes of shorelines. In this study, the results of extracted shorelines of 11 classifiers were validated by using a reference shoreline provided by the local authority. Specifically, the validation assessment was performed using Mean Shoreline Change method to examine the differences between the extracted shorelines and the reference shoreline. The research findings showed that SVM Linear attained the highest number of transects and the lowest mean distances between extracted shorelines and reference shoreline, thus rendering it as the most effective image classification technique in demarcating land and water classes. Furthermore, the findings showed that the accuracy of the extracted shoreline was not directly proportional to the accuracy of the image classification, and smoothing operation using PAEK affected the quality of extracted shorelines. Moreover, the tolerance setting that was ten times the spatial resolution of satellite images was observed to be the most optimal configuration.**

***Index Terms*— Image classification; Medium resolution satellite image, Shoreline extraction; Validation assessment.**

I. INTRODUCTION

Coastal zones are constantly exposed to natural processes and anthropogenic activities that are continually reshaping and redefining the coastal areas of countries on a massive, unpredictable scale[1]. Thus, the monitoring of coastal zones provides important information about prevailing conditions of coastal areas resulting from natural and human activities. In fact, such conditions can be monitored by examining the changes occurring at shorelines of coastal areas. Essentially, a shoreline is an interface that physically separates land and water, effectively creating a boundary between the two [2]. As such, the extraction of shorelines helps provide historical records of physical changes that have taken place, which are useful for prediction purposes. Irrespective of the nature of coastal areas, acquiring a shoreline entails a shoreline indicator that represents the true position of a boundary [3].

In view of the importance of shorelines in such monitoring, this study was carried out to determine and validate the most effective machine learning technique for the extraction of shoreline of the North West coast of Peninsular Malaysia based on a Landsat OLI satellite image. This study was based on Syaifulnizam Abd Manaf et al.'s [4] study, but the former focused on the use and validation of pixel-based approaches to classify land-water classes for the extraction of shorelines using 11 different machine learning classifiers. More importantly, the extracted shorelines were compared with a reference shoreline to identify the most suitable machine learning technique for extracting shorelines. Additionally, the researchers examined the accuracy of image classifications of discriminating classes in the extraction process.

To facilitate discussion, this paper is structured as follows: Section II discusses the related works, Section III details the methodology used, Section IV reports the experimental results, including the satellite image classifications and the validation of the machine learning techniques, Section V highlights the main discussion of the paper, and Section VI summarizes the main points of the paper.

II. RELATED WORKS

Currently, many techniques have been used to extract shorelines from optical multispectral satellite images. Such techniques include image processing techniques, image classification techniques, and spectral bands techniques, which are briefly discussed as follows:

A. Image Processing Techniques

The image processing techniques include segmentation[5], edge detection[6] and wavelet[7] techniques, which are used to delineate shorelines from satellite images.

B. Machine Learning

Fundamentally, the satellite image classification techniques based on machine learning can be divided into two types of classifications: (i) supervised classification, such as Maximum Likelihood, Mahalanobis Distance, Minimum Distance, Neural Network and Support Vector

Machines[8][9][10] and (ii) unsupervised classification, such as ISODATA[9].

C. Spectral Bands Techniques

For spectral bands techniques, band rationing[11][12], normalized difference vegetation index (NDVI) [13] normalized difference water index (NDWI)[14] are some of the techniques commonly used to establish boundaries that differentiate the land from the water. Given the varying extraction techniques, the researchers used a number of supervised classifiers to assess extracted shorelines of a particular study area by comparing them with a reference shoreline.

For the extracted shoreline vector validation techniques, Digital Shoreline Analysis System (DSAS) [9][15] is commonly used as the validation tool. In contrast to previous studies involving DSAS with single baseline, this research used AMBUR with double baselines to validate such extraction techniques. Moreover, this research also focused on the smoothing process performed on the extracted shorelines using different configuration settings.

III. Materials And Methods

The method used to extract shorelines from satellite images consisted of five phases, namely pre-processing, satellite image classification, accuracy assessment, post-processing, and validation assessment, as depicted in Figure 1.

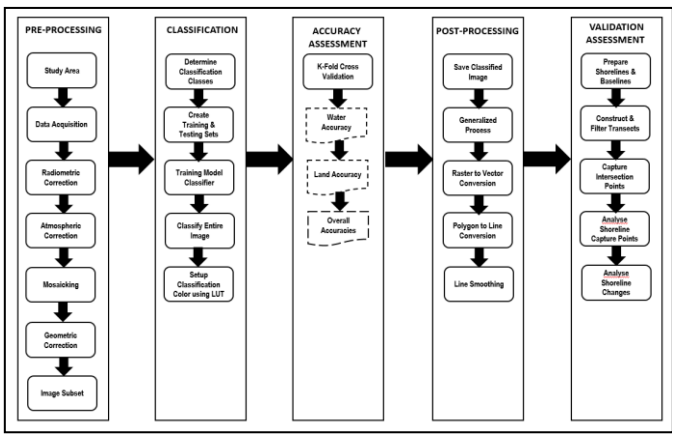

Figure 1: The five phases of the shorelines extraction method of the study

A. Pre-processing

The pre-processing phase involved identifying a specific study area and acquiring data before performing other error cleaning processes, such as radiometric correction, atmospheric correction and geometric correction. In addition, mosaicking was performed on the acquired image, which formed a subset of the study area.

1) Study Area

The chosen study area was the Langkawi Island, which is located at the North West coast of Peninsular Malaysia, as shown in Figure 1. Geographically, this island is located at 6º 15'N and 6º 29'N latitude and 99º 37'E and 99º 57'E longitude, covering a total area of about 47,848 ha. In 1987, this island gained a duty-free status, thus propelling it to become a major tourist destination [16]. Interestingly, this resort island comprises many small islands; however, only the main landmass was considered in this study.

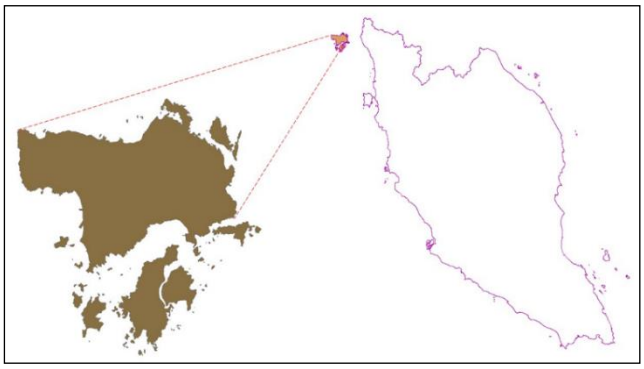

Figure 2: The study area of research

2) Data Acquisition

In this study, the data used were multispectral Landsat-8 Operational Land Imager (OLI) images. The images (which were acquired on 4 and 11 March 2016) were used because they provided sufficient area for such a study. Moreover, the combination of two images helped reduce the covering of clouds that obfuscated the study area, thus improving the quality of extraction process.

3) Radiometric Correction

This process helped calibrate the digital number (DN) values of the satellite image to radiance (Lλ), as expressed by Equation (1).

$$L\lambda = Gain * Pixel\ value + Offset \quad (1)$$

The pixel value ranges from "0" to "255", and the radiance for each image band depends on the gain and offset values.

4) Atmospheric Correction

After calibrating the image data, the atmospheric correction method converted the image radiance to image reflectance. Essentially, the reflectance image is the ratio between the reflected energy and the incident energy on a surface. In this research, Dark Object Subtraction (DOS)[17] method was applied to cancel out the haze component caused by atmospheric absorption and scattering effects of the satellite image data [18]. This process uses the minimum value of a band, which represents the background signature of the band.

5) Mosaicking

Mosaicking process was then applied to combine two images of the same scene of the study area into a single large image using a similar coordinate system. In this study, the researchers mosaicked the images using global WGS1984 coordinate system.

6) Geometric Correction

Image registration process was performed using image-to-image geometric correction process with 30 ground control points (GCP) and RMS value of 0.499, as depicted in Figure 3. Later, Rectified Skew Orthomorphic (RSO) Kertau was used to project the image data of the West Coast of Peninsular Malaysia onto a local projection system.

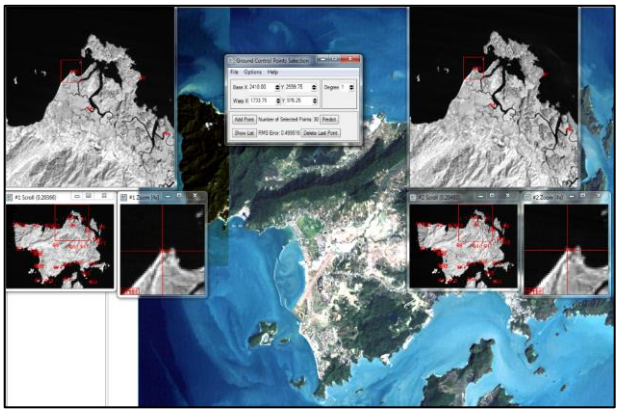

Figure 3: The image-to-image geometric correction process

7) Image Subset

Finally, a small portion of the image rather than the entire scene was selected for further analysis. The image subset was created such that it could fit in with the study area. Furthermore, it could use the local coordinate system to align data together to form a single map.

B. Satellite Image Classification

In the classification phase, pixel-based supervised classification approaches were used with Python Scikit-learn 0.18 machine learning packages to classify land and water classes of the satellite images. For this study, 11 different machine learning classifiers were used, namely Decision Tree (DT), Naïve Bayes (NB), k-Neareast Neighbour (kNN), Linear Discriminat Analysis (LDA), Quadratic Discriminant Analysis (QDA), Logistic Regression (LR), SGD Classifier, Multilayer Perceptron (MLP), SVM-Linear (SVM-L) , SVM-RBF (SVM-R), and SVM-Polynomial (SVM-P).

Figure 4: Training and testing sets of study area

A training set was created to build the model for which a testing set was developed to test its performance. For this study, the training and testing sets consisted of 200 instances, with 100 polygon-format instances generated for each land class and each water class, as shown in Figure 4.

C. Accuracy Assessment

In the accuracy assessment phase, the overall classification accuracy was used as initial measurement indicators. In addition, land and water accuracies were assessed to determine the most suitable classifier for extracting land class or water class or both. Clearly, the selection of machine learning classifiers depends on the classification accuracy. As such, the overall accuracy was used as the primary performance indicator, because it is widely used in the evaluation of satellite image classification methods. For cross validation, the 10-fold cross-validation method was used to address overfitting of classified image.

D. Post-processing

In the post-processing phase, the resultant classified image underwent a conversion process to GIS vector format using ENVI 5.3, which would be further processed using ArcGIS 10.3. Subsequently, after saving the classified images to a hard drive, sieve and clump processes were performed to smoothen the resultant polygons of the classified image. Then, this image underwent a raster-to-vector conversion process to produce an image based on GIS vector format. Later, the polygon-to-line conversion process was carried out to ensure the image would only consist of lines based. Finally, line smoothing using Polynomial Approximation with Exponential Kernel (PAEK) method was applied on the final shoreline after all erroneous data were removed.

E. Validation Assessment

Finally, in the validation phase, AMBUR [19] was used to validate the extracted shorelines against a reference shoreline (which was acquired in 2016 from the local authority). Accordingly, the shorelines were merged with the reference shoreline to form a single shoreline data, with which each extracted shoreline from machine-learning algorithm was analyzed using AMBUR. In fact, screen digitizing was used to create two baselines that covered both the interior and the exterior of the shorelines. The use of two baselines is better than the use of a single baseline as the former helps improve transects orientation of curved shorelines [19]. Furthermore, the shapes of baselines are important for the calculations of changing shorelines that will influence transects orientation [19]. Cast transects were then constructed along the border of shorelines, which were demarcated by the outer and inner baselines. The distances from the transects' starting points to the extracted shorelines' transecting points were then calculated. Lastly, the change between the extracted shoreline and the reference shoreline was calculated using Mean Shoreline Change[19] or Net Shoreline Movement (NSM) in DSAS [20] as shown in Equation (2).

$$Mean\ Shoreline\ Change = \left(\frac{y_{reference} - y_{extracted}}{x_{reference} - x_{extracted}}\right) \quad (2)$$

The numerator is the difference in the distance between the reference shoreline and the extracted shoreline in *y* direction, and the denominator is the difference in the distance between the reference shoreline and the extracted shoreline in *x* direction.

The first performance measure of the classifiers was based on the total number of transects, with higher numbers indicating better performance. The second performance measure of the classifiers was based on the mean distance [9],

with values approaching zero ("0") to be indicative of good performance. In addition, the mean distance between seawater (+ve) and land (–ve) was used as the third performance measure, with lower values indicating better performance.

IV. EXPERIMENTAL RESULTS

A. *Satellite Image Classification Results*

Table 1 summarizes the results of satellite image classification using single classifiers. Clearly, with an overall accuracy of 100%, SVM-P was the best classifier; in contrast, with an overall accuracy of 99.55%, QDA was deemed the least effective classifier. In addition, the remaining classifiers attained relatively high overall accuracies, ranging from 99.71% (for LDA) to 99.97% (for DT). Interestingly, all classifiers achieved land and water accuracies of more than 99%. On closer examination, SVM-P and DT were the two most effective classifiers for classifying land, with each registering land accuracy of 100%. Table 1 summarizes the land, water, and overall accuracies of the 11 classifiers. The results of land and water accuracies, as shown Table 1, were actually extracted from the confusion matrix table of each classifier. For example, Table 2 highlights the confusion matrix of QDA.

Table 1
The land, water and overall accuracies of satellite image classifications using single classifiers

ML Classifiers	Land Accuracy	Water Accuracy	Overall Accuracies
DT	100.00	99.96	99.97
NB	99.82	99.69	99.73
KNN	99.92	99.96	99.95
LDA	99.53	99.78	99.71
QDA	99.88	99.42	99.55
LR	99.68	99.82	99.77
SGD	99.55	99.82	99.74
SVM-L	99.82	99.78	99.79
SVM-R	99.98	99.95	99.96
SVM-P	100.00	100.00	100.00
MLP	99.84	99.94	99.91

As shown in Table 2, the confusion matrix was used to measure the performance of ML classifiers based on their 16,403 predictions. Evidently, QDA predicted land 4,993 times and water 11,410 times; out of these, 4,932 predictions belonged to the land class, while 11,471 predictions belonged to the water class.

Table 2
The confusion matrix result of QDA Classifier

Predict / Truth	Land	Water	Total	Accuracy
Land	4926	6	4932	99.88
Water	67	11404	11471	99.42
Total	4993	11410	16403	

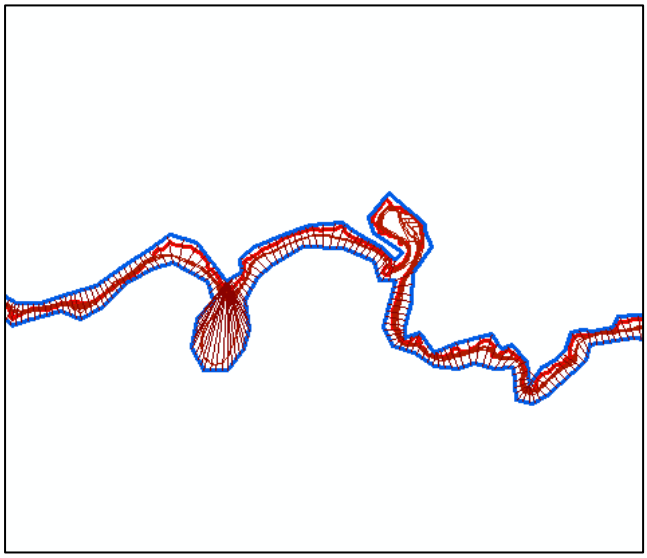

Figure 5: The extracted shorelines, baselines, and transects after the validation process

B. *Shoreline Validation Results*

Figure 5 shows the extracted shorelines (of the 11 machine-learning classifiers), baselines, and transects after the validation assessment process. The figure shows the inner and the outer baselines distinguishing the extracted shorelines from the reference shoreline, as highlighted by various line colors. For example, the blue, red, and brown lines represent the baselines, shorelines, and transects, respectively.

a) Validation of Original Extracted Shorelines

Table 3 summarizes the results of validation of the original extracted shorelines. As shown, SVM-L had the lowest number of instances, with 35 instances of vector polylines data only, making it as an effective technique (which is based on a smooth raster-to-vector post-processing) to achieve simple separation of land and seawater classes. On the other hand, SVM-R had the highest number of instances, with 87 instances of vector polylines, establishing it to be the least effective technique, given the complex separation of the two classes.

Table 3
The results of the validation assessment of original extracted shorelines using 11 ML classifiers without PAEK

ML Classifiers	No of Instances	Transects	Mean	Mean (+)	Mean (-)
DT	51	2,941	13.15	36.62	-22.73
NB	65	2,937	21.72	43.41	-22.33
KNN	71	2,947	4.15	30.38	-31.07
LDA	81	2,917	-9.78	30.84	-41.81
QDA	67	2,932	27	46.51	-18.43
LR	60	2,935	-4.82	30.37	-36.57
SGD	61	2,943	0.97	34.15	-37.35
SVM-L	35	2,948	2.5	30.96	-31.65
SVM-R	87	2,946	14.06	35.58	-27.49
SVM-P	53	2,941	13.16	36.64	-22.73
MLP	75	2,932	14.66	39.44	-23.68

Table 3 shows the number of transects on the interval of 500 m generated from the ML classifiers, ranging from 2,917 to

2,948. These transects separated the land classes from the water classes to form several different boundaries, which are known as shorelines. As shown, SVM-L recorded had the highest number with 2,948 transects, while LDA had the lowest number with 2,917 transects. As such, the former was the most effective classification technique for shoreline extraction; in contrast, the latter was the least effective classification technique. The result showed SVM-L generated 2,948 transects, which was closest to the reference shoreline that generated 2,959 transects. The second and third performance measurements were not performed on the original data, as only SVM-L had the number of transects closest to the reference shoreline. Interestingly, SGD recorded the smallest mean score (approaching zero), which might render it as the most effective classifier. However, SGD's number of transects was slightly less than SVM-L's, thus elevating the latter to the top spot as the most effective classifier among the 11 classifiers.

b) Validation of Smoothened Extracted Shorelines with PAEK

Table 4 summarizes the results of validation of extracted shorelines after performing the smoothing process using PAEK with different tolerance configurations, as shown in Figure 6.

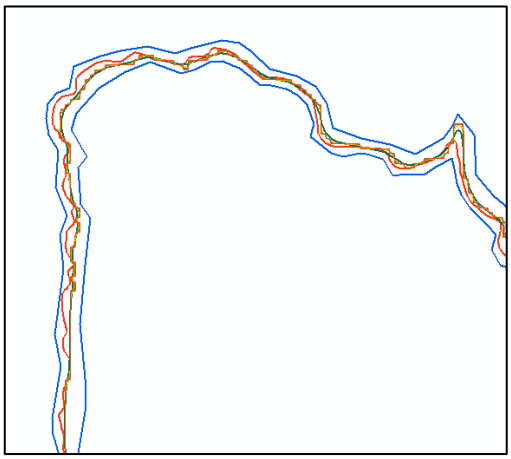

Figure 6: The comparison between original and smoothened extracted shorelines using SVM-L

In general, the number of transects of ML classifiers increased with increasing tolerance settings, ranging from 30 m to 300 m. Notably, at the initial setting of 30 m, six classifiers, namely DT, NB, QDA, SVM-R, SVM-P and MLP, were observed to have slightly lower numbers of transects compared with the number of transects of the original extracted shorelines. For the remaining classifiers, the numbers of transects either remained the same or increased slightly at this initial tolerance setting. Furthermore, the maximum tolerance setting was 300 m, as the numbers of transects of some classifiers tended to decrease at this setting and beyond. Obviously, the classifiers had reached the optimal tolerance setting at 300 m. Quite surprisingly, at this maximum setting, three classifiers failed to achieve the maximum number of transects (i.e., 2,959), namely DT, LDA and SVM-P.

The second and third performance indicators were then considered after almost all the classifiers had reached the optimal number of transects. In general, the use of PAEK helped decrease the mean scores of classifiers with increasing tolerance setting. However, such a decreasing trend was not observed for two classifiers, namely LDA and LR, as their mean scores tended to increase.

Table 4
The number of transects of smoothened extracted shorelines using PAEK, with different tolerance settings

ML	Original	T=30	T=60	T=90	T=150	T=300
DT	2,941	2,938	2,945	2,952	2,955	2,958
NB	2,937	2,935	2,938	2,939	2,951	2,959
KNN	2,947	2,947	2,951	2,954	2,958	2,959
LDA	2,917	2,920	2,926	2,936	2,949	2,958
QDA	2,932	2,930	2,931	2,937	2,945	2,959
LR	2,935	2,942	2,942	2,947	2,956	2,959
SGD	2,943	2,947	2,947	2,952	2,956	2,959
SVM-L	2,948	2,949	2,951	2,956	2,959	2,959
SVM-R	2,946	2,944	2,951	2,956	2,959	2,959
SVM-P	2,941	2,938	2,945	2,952	2,955	2,958
MLP	2,932	2,931	2,936	2,939	2,945	2,959

As shown in Table 8, at the tolerance setting of 300 m, SVM-L recorded a mean score of 0.26 m (which was closest to zero), thus making it the most effective classifier based on this measure. Likewise, KNN and SGD were also deemed highly effective based on their relatively low mean scores of 1.44 m and -1.81 m, respectively. In contrast, NB and QDA were least effective, given their low mean scores of 18.04 m and 23.97 m, respectively. Surprisingly, DT, LDA and SVM-P failed to achieve the maximum number of transects required, and hence they were not considered for further analysis.

Table 5
The overall mean scores of the original extracted shorelines and smoothened extracted shorelines using PAEK based on different tolerance settings

ML	Original	T=30	T=60	T=90	T=150	T=300
DT	13.15	12.36	12.29	11.67	10.77	9.57
NB	21.72	21.10	20.53	20.65	20.05	18.04
KNN	4.15	3.67	3.72	3.54	2.44	1.44
LDA	-9.78	10.11	-10.23	-10.36	-11.63	-13.32
QDA	27.00	26.28	26.27	25.84	25.11	23.97
LR	-4.82	-5.31	-5.08	-5.19	-6.48	-7.95
SGD	0.97	0.31	0.39	0.41	-0.59	-1.81
SVM-L	2.50	2.08	2.26	2.33	1.28	0.26
SVM-R	14.06	13.57	13.81	13.9	13	11.96
SVM-P	13.16	12.37	12.30	11.68	10.78	9.57
MLP	14.66	13.92	13.86	13.28	12.31	11.15

Table 6 shows the overall mean distances between seawater (+ve) of the original extracted shorelines and smoothened extracted shorelines as generated by the 11 classifiers with PAEK. Clearly, such mean distances tended to decrease with increasing tolerance setting, except for LDA and LR that had negative overall mean distances. Evidently, at the tolerance setting of 300 m, KNN, LR and SVM-L were the top three effective classifiers, as their positive mean distances were roughly 30 m, which were far smaller than others were. By contrast, QDA, NB, and MLP were deemed

least effective classifiers, given their relatively higher mean distances of roughly 40 m.

Table 6
The overall mean distance between seawater (+ve) of the original extracted shorelines and smoothened extracted shorelines using PAEK based on different tolerance settings

ML	Original	T=30	T=60	T=90	T=150	T=300
DT	36.62	35.75	35.28	33.63	33.57	33.76
NB	43.41	42.80	41.61	41.55	41.85	40.69
KNN	30.38	29.77	29.61	29.02	28.91	29.63
LDA	30.84	30.37	30.28	29.98	30.28	30.89
QDA	46.51	45.60	45.22	44.15	44.27	44.91
LR	30.37	29.85	30.08	29.55	29.95	30.31
SGD	34.15	33.48	33.55	33.41	33.66	34.83
SVM-L	30.96	30.34	30.42	30.18	29.97	30.6
SVM-R	35.58	35.00	34.76	34.53	34.12	34.74
SVM-P	36.64	35.76	35.29	33.65	33.59	33.76
MLP	39.44	38.38	38.05	36.39	36.42	37.01

Table 7 shows the overall mean distances between land (-ve) of the original extracted shorelines and smoothened extracted shorelines as generated by the 11 classifiers with PAEK. Clearly, such mean distances tended to increase with increasing tolerance setting, except for MLP that tended to decrease. Evidently, at the tolerance setting of 300 m, QDA, NB, and MLP were the top three effective classifiers, as their negative mean distances were roughly -20 m, which were far smaller than others were. On the other hand, LDA, LR, and SGD were deemed least effective classifiers, given their relatively higher negative mean distances of roughly -40 m.

Table 7
The overall mean distance between land (-ve) of the original extracted shorelines and smoothened extracted shorelines using PAEK based on different tolerance settings

ML	Original	T=30	T=60	T=90	T=150	T=300
DT	-22.73	-22.77	-22.24	-22.42	-23.20	-25.03
NB	-22.33	-22.14	-21.98	-21.52	-21.47	-22.4
KNN	-31.07	-30.99	-30.18	-30.1	-30.4	-31.18
LDA	-41.81	-41.7	-41.47	-41.28	-42.12	-43.58
QDA	-18.43	-18.43	-18.02	-17.44	-18.14	-19.24
LR	-36.57	-36.59	-35.59	-35.65	-36.4	-38.02
SGD	-37.35	-37.61	-36.95	-36.68	-37.18	-38.13
SVM-L	-31.65	-31.62	-30.69	-30.17	-30.8	-31.97
SVM-R	-27.49	-27.54	-26.96	-26.43	-27.22	-29.11
SVM-P	-22.73	-22.77	-22.24	-22.42	-23.2	-25.03
MLP	-23.68	-23.59	-22.97	-22.57	-22.8	-23.28

As shown in Table 8, SVM Linear was the most effective classification technique for the shoreline extraction based on three performance measures. Specifically, it had the highest number of transects with 2,959 instances, the lowest mean distance of only .25 m, and the third lowest mean +ve distance, as compared to other classifiers. Similarly, KNN and SGD were also held to be reasonably effective, given their relatively low mean distances of 1.44 m and -1.81 m, respectively. These mean distances, which were well below ±5 m from the reference shoreline, are quite acceptable for this domain study.

Table 8
The results of validation assessment of smoothened extracted shorelines using PAEK with tolerance setting of 300 m

ML Classifiers	Transects	Mean	Mean (+)	Mean (-)
DT	2,958	9.57	33.76	25.03
NB	2,959	18.04	40.69	22.40
KNN	2,959	1.44	29.63	31.18
LDA	2,958	-13.32	30.89	43.58
QDA	2,959	23.97	44.91	19.24
LR	2,959	-7.95	30.31	38.02
SGD	2,959	-1.81	34.83	38.13
SVM-L	2,959	0.26	30.60	31.97
SVM-R	2,959	11.96	34.74	29.11
SVM-P	2,958	9.57	33.76	25.03
MLP	2,959	11.15	37.01	23.28

By contrast, DT, LDA, and SVM-P were the least effective classification techniques, as attested by their low numbers of transects that precluded further analysis. In addition, QDA was deemed as an ineffective technique, because of its high mean distance of 23.97 m. Equally less effective were LR, SVM-P, and DT, as evidenced by their relatively low mean distances, which were well below ±10 m from the reference shoreline. Their mean distances to the sea (+ve transects) were recorded between 29.63 m and 44.91 m, while their mean distances to the land (-ve transects) were recorded between 19.24 m and 43.58 m.

V. DISCUSSIONS

A. Discussions

In this study, 11 single machine-learning classifiers were used to perform a series of validation assessments on extracted shorelines. To achieve a precise extracted shoreline, the researchers had to perform a change analysis on the extracted shorelines with the reference shoreline. There were 2,959 cast transects used to cover the reference shoreline, stretching 163.7 km in length. Predictably, such classification techniques used to compare the distance between the extracted shoreline and the reference shoreline (which was generated from GPS data of a field survey provided by the local authority) had resulted in differences in the distance between those shorelines. In fact, the mean distance between seawater and land was approximately 30 m due to the spatial resolution of Landsat 8, which was 30 m. From the analysis carried out, SVM Linear was the most effective technique for extracting shorelines, as qualified by the high number of transects, the lowest mean distance between seawater and land of only .26 m, and the small deviations in the measurement of distance to seawater (+ve transect) and to land (-ve transect) of ±30 m. Therefore, practitioners should use this machine-learning classifier to help extract accurate shorelines of islands or landmass.

VI. CONCLUSION

In this study, the researchers carried out a series of validation assessments of extracted shorelines based 11 single

machine-learning classifiers with PAEK algorithm. This algorithm helped smoothen the extracted shorelines that would improve the extraction process. To determine the effectiveness of the classifiers, a change analysis was performed on the extracted shorelines with a reference shoreline (which was generated from GPS data of a field survey provided by the local authority). The image extraction generated 2,959 cast transects to cover the reference shoreline that stretched roughly 163.7 km. The analysis revealed that SVM Linear was the most effective classifier for extracting shoreline; in contrast, QDA was found to be the least effective classifier. Such different performances among the classifiers were attributed to the different machine-learning algorithms used in calculating the difference in distance between land and water classes. More specifically, the effectiveness of classifiers was based on three criteria, namely the number of transects, the mean distance between seawater and land, and the deviation in the mean distance.

For future research, other classification techniques, such as DSAS that uses single baseline, could be utilized to perform the change analysis. The results of the analysis could then be compared with AMBUR that uses double baseline. In addition to using supervised satellite image classification using machine learning, shoreline extraction could be compared with other new techniques, such as ISODATA unsupervised classification, and spectral methods, such as Normalize Difference Vegetation Index (NDVI) and Normalize Difference Water Index (NDWI).

ACKNOWLEDGMENT

The authors would like to thank the Ministry of Science, Technology and Innovation of Malaysia for the Science Fund Research Grant (No: 01-01-04-SF2291), the Malaysian Remote Sensing Agency, the Department of Survey and Mapping of Malaysia, the Federal Department of Town and Country Planning Peninsular Malaysia, and the United States' Geological Survey, and Universiti Putra Malaysia. In addition, the authors would like to thank the National Hydraulic Research Institute of Malaysia for the data and technical support rendered.

REFERENCES

[1] M. F. Mohamad, L. H. Lee, and M. K. H. Samion, "Coastal Vulnerability Assessment towards Sustainable Management of Peninsular Malaysia Coastline," *Int. J. Environ. Sci. Dev.*, vol. 5, no. 6, pp. 533–538, 2014.

[2] E. H. Boak and I. L. Turner, "Shoreline Definition and Detection: A Review," *Journal of Coastal Research*, vol. 214. pp. 688–703, 2005.

[3] R. Gens, "Remote sensing of coastlines: detection, extraction and monitoring," *Int. J. Remote Sens.*, vol. 31, no. 7, pp. 1819–1836, 2010.

[4] Syaifulnizam Abd Manaf, Norwati Mustapha, Md. Nasir Sulaiman, Nor Azura Husin, and Mohd Radzi Abdul Hamid, "Artificial Neural Networks for Satellite Image Classification of Shoreline Extraction for Land and Water Classes of the North West Coast of Peninsular Malaysia," *Adv. Sci. Lett.*, vol. 4, no. 2, pp. 400–407, 2016.

[5] S. M. Semenov, N. A. Abushenko, and A. S. Chichigin, "Discrimination of Shorelines on Satellite Images from Boundary-Point and Halftone Information," *Mapp. Sci. Remote Sens.*, vol. 36, no. 4, pp. 245–255, 2016.

[6] Y. Zhang, X. Li, J. Zhang, and D. Song, "A Study on Coastline Extraction and Its Trend Based on Remote Sensing Image Data Mining," *Abstr. Appl. Anal.*, vol. 2013, no. Article ID 693194, p. 6, 2013.

[7] S. Yu, Y. Mou, D. Xu, X. You, L. Zhou, and W. Zeng, "A New Algorithm for Shoreline Extraction from Satellite Imagery with Non-separable Wavelet and Level Set Method," *Int. J. Mach. Learn. Comput.*, vol. 3, no. 1, pp. 158–163, 2013.

[8] K. Rokni, A. Ahmad, K. Solaimani, and S. Hazini, "A new approach for surface water change detection: Integration of pixel level image fusion and image classification techniques," *Int. J. Appl. Earth Obs. Geoinf.*, vol. 34, no. September, pp. 226–234, 2015.

[9] I. Sekovski, F. Stecchi, F. Mancini, and L. Del Rio, "Image classification methods applied to shoreline extraction on very high-resolution multispectral imagery," *Int. J. Remote Sens.*, vol. 35, no. 10, pp. 3556–3578, 2014.

[10] A. Yousef and K. Iftekharuddin, "Shoreline extraction from the fusion of LiDAR DEM data and aerial images using mutual information and genetic algrithms," *Proc. Int. Jt. Conf. Neural Networks*, pp. 1007–1014, 2014.

[11] C. Lira and R. Taborda, *Advances in Applied Remote Sensing to Coastal Environments Using Free Satellite Imagery*. 2014.

[12] M. G. M. Sarwar and C. D. Woodroffe, "Rates of shoreline change along the coast of Bangladesh," *J. Coast. Conserv.*, vol. 17, no. 3, pp. 515–526, 2013.

[13] A. Mukhopadhyay, S. Mukherjee, S. Mukherjee, S. Ghosh, S. Hazra, and D. Mitra, "Automatic shoreline detection and future prediction: A case study on Puri coast, Bay of Bengal, India," *Eur. J. Remote Sens.*, vol. 45, no. 1, pp. 201–213, 2012.

[14] Y.-J. Choung and M.-H. Jo, "Shoreline change assessment for various types of coasts using multi-temporal Landsat imagery of the east coast of South Korea," *Remote Sens. Lett.*, vol. 7, no. 1, pp. 91–100, 2016.

[15] N. Tarmizi, A. M. Samad, M. Safarudin, C. Mat, M. Shukri, and M. Yusop, "Qualitative and Quantitative Assessment on Shoreline Data Extraction from Quickbird Satellite Images," *IPASJ Int. J. Comput. Sci.*, vol. 2, no. 9, pp. 54–62, 2014.

[16] N. Samat, "Assessing Land Use Land Cover Changes in Langkawi Island : Towards Sustainable Urban Living," *Malaysian J. Environ. Manag.*, vol. 11, no. 1, pp. 48–57, 2010.

[17] P. S. Chavez, "An improved dark-object subtraction technique for atmospheric scattering correction of multispectral data," *Remote Sens. Environ.*, vol. 24, no. 3, pp. 459–479, 1988.

[18] S. Gilmore, A. Saleem, and A. Dewan, "Effectiveness of DOS (Dark-Object Subtraction) method and water index techniques to map wetlands in a rapidly urbanising megacity with Landsat 8 data," *CEUR Workshop Proc.*, vol. 1323, no. March, pp. 100–108, 2015.

[19] C. W. Jackson, C. R. Alexander, and D. M. Bush, "Application of the AMBUR R package for spatio-temporal analysis of shoreline change: Jekyll Island, Georgia, USA," *Comput. Geosci.*, vol. 41, pp. 199–207, 2012.

[20] A. Thieler, E.R., Himmelstoss, E.A., Zichichi, J.L., and Ergul, "Digital Shoreline Analysis System (DSAS) version 4.0— An ArcGIS extension for calculating shoreline change," 2009.